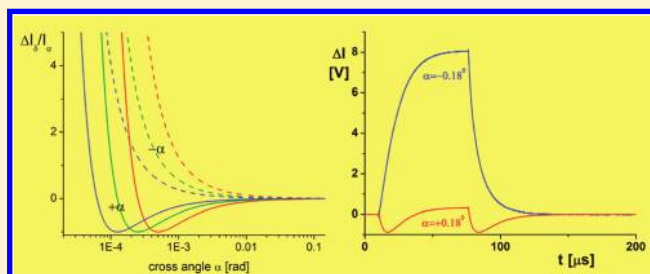


Electric Birefringence at Small Angles from Crossed Position: Enhanced Sensitivity and Special Effects

Dietmar Porschke*

Max Planck Institut für biophysikalische Chemie, AG Biomolecular Dynamics, Am Fassberg 11, 37077 Göttingen, Germany

ABSTRACT: Measurements of electric birefringence with increased sensitivity are possible using lasers with high intensity and stability, provided that perturbations resulting from stray light and strain in cell windows can be reduced. A new type of cell window is designed for minimal strain and is used in a standard birefringence setup with optimized components. The new instrument is characterized by a stray-light constant of 2×10^{-7} and a negligible residual birefringence. Thus, measurements can be extended to small angles from the crossed position providing birefringence signals of high amplitudes at favorable signal-to-noise ratios. Special effects at small angles from the crossed position like a divergent increase of relative amplitudes to extreme values, a nonlinear response, a new type of electro-optical anomaly, and a simple bypass around this anomaly are observed and shown to be consistent with the theory. The technique proves to be particularly useful for measurements at physiological salt concentrations, where signals for most systems are too small under conventional conditions.



INTRODUCTION

Electric birefringence is known to provide useful information for the characterization of global structures and their dynamics in solution.^{1–4} However, standard instruments can be used only at low salt concentrations in the range around 1 mM. Most objects of interest are polyelectrolytes, and thus, their structure is usually dependent on the ionic strength. In many cases, native structures can be expected only at salt concentrations around 100 mM. Thus, applications of electric birefringence have been seriously restricted.

Previous attempts to remove restrictions were focused in this laboratory on the closely related technique of the electric dichroism, using cable discharges for generation of short pulses of high voltage. An instrument⁵ based on this technique was useful for investigation of DNA fragments⁶ and of some proteins,⁷ but again there are limitations, partly because of the high voltages and the short pulses.

In principle, the sensitivity of birefringence measurements can be increased simply by increasing the light intensity and reducing the angle between the polarization planes of polarizer and analyzer. However, usually there are some artifacts resulting for example from cell windows under residual strain and the amplitude of these artifacts increase with the light intensity. For this reason, the main part of the task is construction of all optical components, in particular the cell windows, in an optimal, strain-free state. A new type of cell window is described, which proves to be useful. The selection of the other optical components and their optimal alignment is also essential for an increased sensitivity. Finally, the utility of the new instruments is demonstrated by various experiments under extreme conditions. The potential of this technique

must be used with special care, because some effects can be misleading and corrections for nonlinearity may be necessary.

BIREFRINGENCE EQUATIONS

The electric birefringence records the optical anisotropy generated by an external electric field using polarized light. The anisotropy is measured by a beam of light passing a polarizer, the sample and an analyzer; the polarization planes of the analyzer and the polarizer are in almost perpendicular position. When a perfect polarizer is placed in a polarized beam of light, the intensity I_α of the light that passes through is given by

$$I_\alpha = I_0 \sin^2(\alpha) \quad (1)$$

where I_0 is the initial light intensity and α is the angle between the light's initial polarization direction and the axis of the polarizer ("Malus law"). As described by Fredericq and Houssier,¹ for all standard optical arrangements used in birefringence measurements, the plane of polarized light is at an angle of 45° with respect to the field vector. For optimal measurements of the birefringence, a quarter wave plate is inserted between the sample and the analyzer with its slow axis at $3\pi/4$ with respect to the field vector. Under these conditions a field induced birefringence of the sample will be indicated by a change of the light intensity ΔI_δ

$$\frac{\Delta I_\delta}{I_\alpha} = \frac{\sin^2(\alpha + \delta/2) - \sin^2 \alpha}{\sin^2 \alpha} \quad (2)$$

α is the angle from the crossed position of the polarizers, I_α is the

Received: November 25, 2010

Revised: February 19, 2011

Published: March 21, 2011

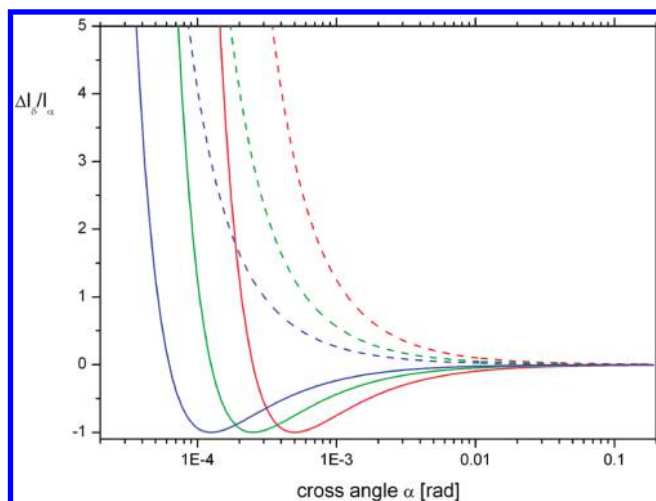


Figure 1. Relative change of the light intensity $\Delta I/I_\alpha$ as a function of the angle α [rad] for different values of the optical retardation δ [rad] according to eq 2: -0.001 (red line), -0.0005 (green line), and -0.00025 (blue line). The dashed lines show the $\Delta I/I_\alpha$ -values for the same retardations (corresponding color code) at “negative” angles α , i.e. angles from crossed position in the opposite direction.

light intensity given at the angle α from the crossed position in the absence of birefringence, and δ is the phase shift or optical retardation resulting from the birefringence.¹

At constant phase shift δ , the change of light intensity $\Delta I/I_\alpha$ increases upon reduction of the angle α between the polarization planes of polarizer and analyzer in a wide range of conditions. Except for very low α -values, a reduction of α by a factor of 2 leads to an increase of the relative change of light intensity $\Delta I/I_\alpha$ by a factor of 2. For an increase of the absolute change of the light intensity by a factor of 2, the loss of light due to the decreased angle α must be compensated by an increase of the input light intensity by a factor of 4. Thus, the sensitivity can be increased by an increase of the light intensity and a simultaneous decrease of the angle α . An increase of the light intensity by a factor of 100 may be used for an increase of the sensitivity by a factor of 10, if the optical conditions are optimal.

This relation remains valid provided that the angle α between polarizer and analyzer is not too close to the crossed position. Equation 2 predicts special effects at low α -values, shown in Figure 1. For a sample with a negative birefringence, the relative change of the light intensity approaches for decreasing α -values first $\Delta I/I_\alpha = -1$, then passes $\Delta I/I_\alpha = 0$, and finally increases to large positive $\Delta I/I_\alpha$ -values. At a given negative optical retardation δ , $\Delta I/I_\alpha = 0$ is found at $\alpha = -\delta/4$. These effects appear for the standard setting of the optical components recommended for measurements at high sensitivity. When the analyzer is turned beyond the crossed position to “negative” α -values, the complex dependence of $\Delta I/I_\alpha$ on α is changed to a relatively simple increase of $\Delta I/I_\alpha$ upon reduction of the “absolute” α -value (cf. Figure 1). Under these conditions (negative birefringence, low α -values) the relative change of light intensity is larger at “negative” α -values.

CONSTRUCTION OF STRAIN-FREE OPTICAL WINDOWS

Perturbations of electric birefringence data mainly result from strain in the optical windows of measuring cells. Strain-free

optical components are required for virtually all optical measurements, but reduction of strain is particularly important for instruments using polarized light. Strain must be reduced to an absolute minimum, when high sensitivities are required. The problems get worse during application of electric field pulses, which usually generate shock waves in the measuring cell and, thus, amplify strain effects.

In many cases birefringence was measured in commercial cuvettes produced for general spectroscopic measurements with homemade inserts for application of electric field pulses. These cuvettes have to be selected for minimal strain. Acquisition of suitable cuvettes was and still is something like lottery winnings.

One of the attempts to get quartz windows in cells used for temperature jumps and/or electric field jumps as strain-free as possible was based on silicon grease: the windows were inserted into the cell body with a layer of grease around them, such that the windows did not have any “hard” contact with the cell body.⁸ A major drawback of this technique was the fact that spreading of the grease to other parts of the cell including the optical surfaces of the cell windows could not be avoided. Grease of high viscosity reduced spreading, but was less effective in damping effects from shock waves. Insertion of cell windows with silicon glue was also used, but changes of temperature induced strain due to different thermal expansion coefficients of quartz and the material used for the cell body.

Because of these difficulties a new form of cell window was constructed. The aim was to avoid direct contact between the quartz window and the cell body. Soft holding of the windows was accomplished by insertion with o-rings made from silicon. For applications with laser light, the windows were reduced to relatively small dimensions. This was useful also for constructing a cell with electrodes at a short distance. The windows were grinded from quartz as rotation cylinders with a stepwise change of the diameter from 6 to 2 mm and cylinder heights of 2 mm for both segments (cf. Figure 2). The planar end surfaces were polished to laser optical quality and were covered with antireflection coating for 532 nm.

Holes complementary to the windows were milled into the cell body made from acrylic glass, with grooves for the silicon o-rings both in the cell body and the holding cylinders. The holding cylinders are inserted by a screw thread and press against the windows via the o-rings at a slight counter pressure (cf. Figure 2). The space milled in the center of the cell body with a cross section of 20×4 mm for the solution was confined bottom-up and top down by Pt-electrodes at a distance of 2.68 mm, defining a cell volume of 215 μL . The goal of the construction is free “floating” of the windows without direct contact to the cell body, held by the silicon o-rings. During loading of the cell with solution, air in the inner space between the quartz and the cell body was removed, when the solution in the cell with mounted lower electrode was freed from air bubbles in a vacuum chamber at a low pressure (slightly below the boiling pressure of water). The upper electrode was mounted as the last step.

COMPONENTS USED FOR THE BIREFRINGENCE OPTICAL SETUP

The currently used light source is a solid-state diode pumped, frequency doubled Nd:vanadate laser (Verdi, Coherent) providing power levels up to 5 W cw at 532 nm. The power level used for standard measurements is 0.5 W. The light beam is carefully adjusted to the standard position and direction by an adjustable

double mirror, guided by a rail from Zeiss. The specified beam diameter is $2.25 \text{ mm} \pm 10\%$. A Galilean telescope with lenses of focal length 200 mm and -30 mm is used to reduce the beam diameter to nominally 0.34 mm. This reduction is simple according to telescope theory and specified initial diameter, but

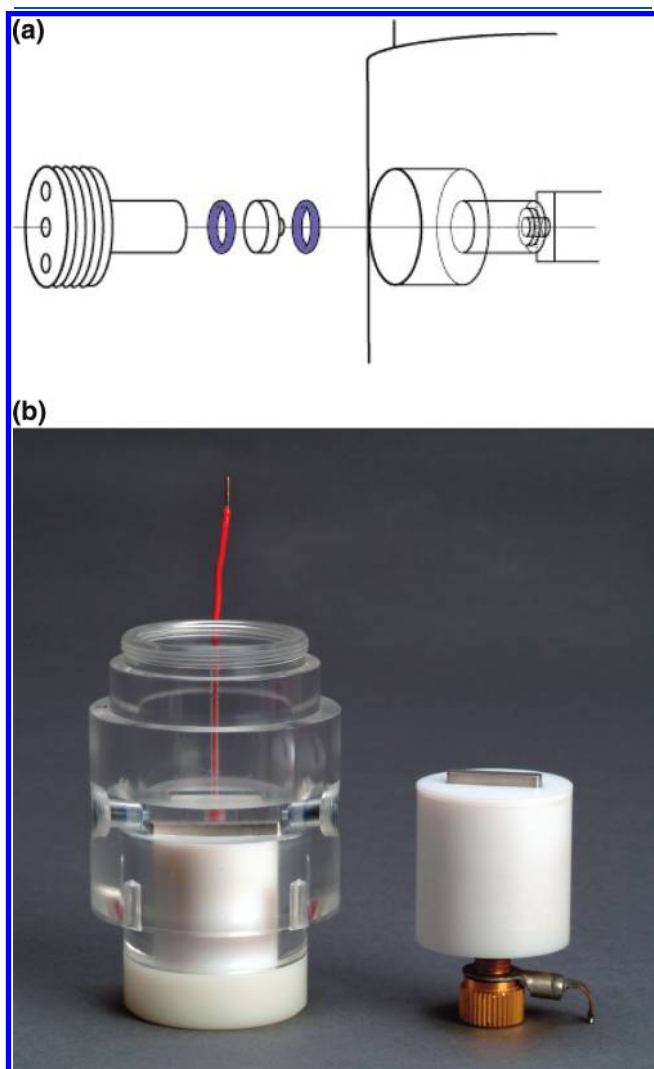


Figure 2. (a) Explosion view of the cell window construction with components (from right to left): cell body from acrylic glass, silicon O-ring, quartz window, silicon O-ring, and holding cylinder from dynal. (b) Photo of the cell with windows and lower electrode assembled. The red cable is the electrical connection to the lower Pt-electrode; the upper Pt-electrode (right), fixed on a dynal cylinder, is constructed similar to the lower one.

turns out to be not so simple in practice and requires a very careful adjustment of the lens system. Commercial adjustable lens holders were hardly sufficient with respect to the required accuracy/stability in the present case. After contraction of the light beam by the telescope, the plane of polarization is rotated to 45° by a half-wave plate and a polarizer aligned at 45° ensures complete polarization. Then the light beam passes the measuring cell, a quarter wave plate, the analyzer and finally hits the detector (Figure 3). As described by Fredericq and Houssier,¹ the rotation of the analyzer is first adjusted in the absence of the quarter wave plate to extinction and then the quarter wave plate is inserted and rotated to restore the initial extinction. Finally, the analyzer is rotated by an angle α from the crossed position toward the polarization plane of the polarizer. α -values corresponding to this standard direction of rotation are given as positive values. Rotation in the opposite direction from the crossed position is denoted by α -values with a negative sign. Polarizers and wave-plates are covered with antireflection coating. The light intensity was measured with a Si photodiode in the photodetector HCA-S from FEMTO Messtechnik GmbH (Berlin). When the response curve of the detector is approximated by an exponential, the time constant is $\sim 100 \text{ ns}$. However, the shape of the response curve is more sigmoidal than exponential and, thus, numerical deconvolution⁹ is the appropriate procedure for evaluation of transients with time constants close to that of the detector. A sigmoidal shape of response curves is usually due to a convolution of more than a single contribution to a delayed detector response.

ELECTRIC FIELD PULSE GENERATION

One of the problems with electro-optical measurements at high salt concentrations is application of high voltage pulses at the given high conductivity. In the present cell construction the conductivity is reduced to a relatively low value by reduction of the cell cross section as much as possible. At the given cell geometry, the resistance of the cell filled with an aqueous 100 mM salt solution is $\sim 70 \text{ Ohm}$ at temperatures around 2°C . This resistance is below the standard specified for Cober pulse generators, but it was still possible to apply dc electric field pulses of sufficient magnitude. The polarity of the pulse was reverted automatically after each pulse by a relay system.

The ac pulses with frequencies around 1 MHz were generated by an arbitrary wave function generator together with a high power pulse amplifier.

MATERIALS

The DNA restriction fragments with 84 and 256 base pairs were prepared as described in ref 6.

The DNA fragment with 549 base pairs was prepared from the plasmid described in ref 10 by the restriction nucleases Ecl136II

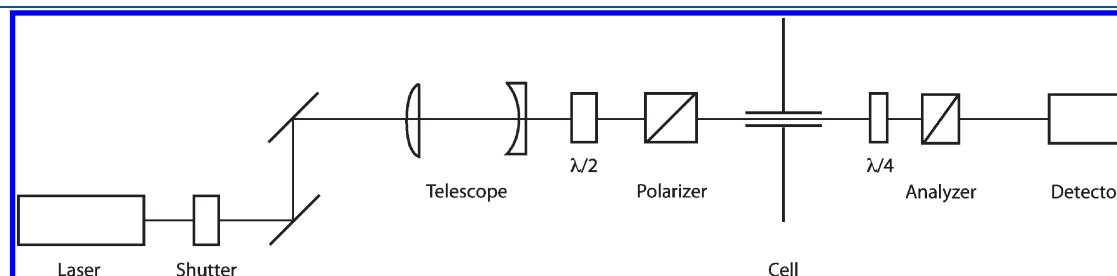


Figure 3. Scheme of the optical setup. For details, see text.

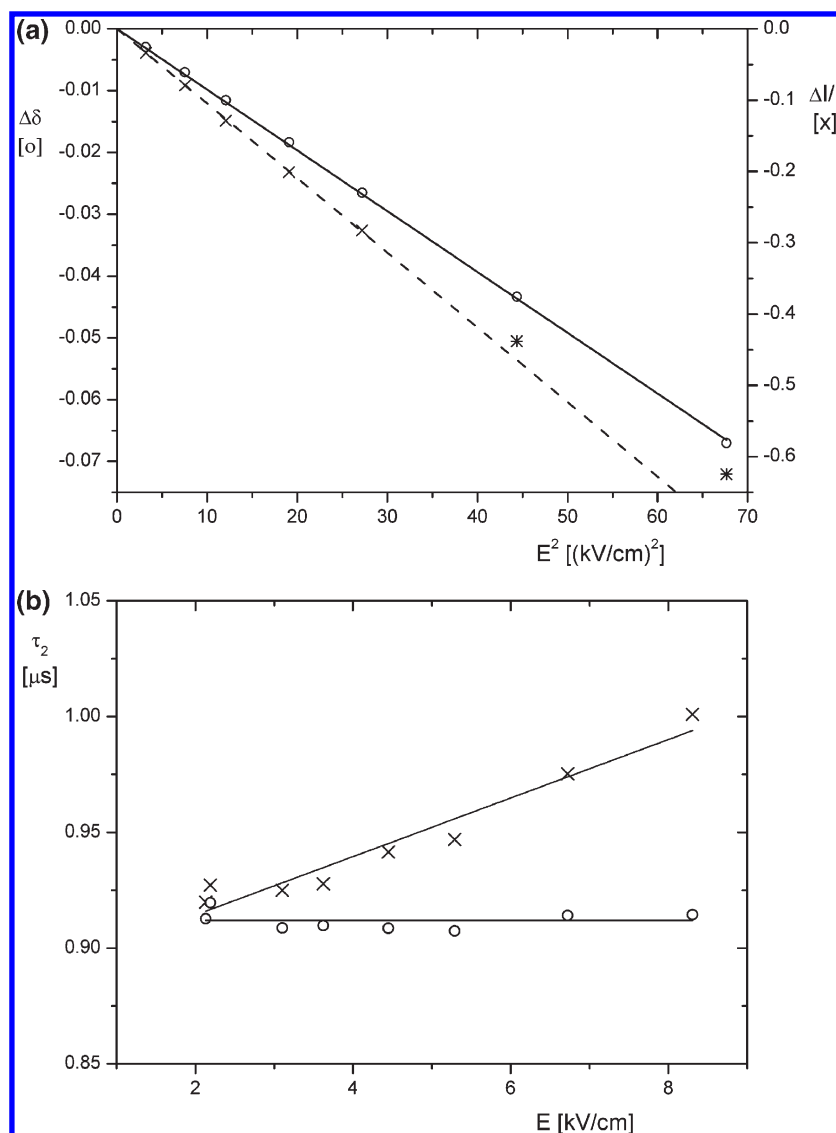


Figure 4. (a) Stationary birefringence amplitudes of 0.138 μM 84 bp DNA in 1 mM NaCl, 1 mM Na-cacodylate pH 7, 0.2 mM EDTA at 2 °C as a function of the square of the electric field strength E^2 : \times and $*$ represent $\Delta I/I$ -values (right scale); the values up to $E \sim 5$ kV/cm follow the Kerr law within the limits of accuracy, whereas clear deviations exist at higher E -values ($*$); the $\Delta I/I$ -values converted to optical retardation $\Delta\delta$ follow the Kerr law up to the high E -values (o, left scale). (b) Birefringence decay time constants of 84 bp DNA in 1 mM NaCl, 1 mM Na-cacodylate pH 7, 0.2 mM EDTA at 2 °C fitted directly to the measured $\Delta I = f(t)$ data (\times) and fitted after conversion of the $\Delta I = f(t)$ data to optical retardation values (o) using eq 2.

and EheI; the fragment was purified by phenol extraction, size exclusion chromatography and finally by preparative gel electrophoresis. The DNA fragments were dialyzed extensively against the buffers used for the measurements. Buffer T contained: 90 mM NaCl, 20 mM Tris pH 8, 0.1 mM EDTA, and 1 mM DTT.

EXPERIMENTAL TESTS

The quality of the optical setup is indicated by the residual light signal measured in the crossed position of the polarizer. For current standard conditions of the new birefringence setup using 0.5 W laser light intensity the stray light constant¹¹ is 2×10^{-7} . Another important parameter is the residual birefringence of the measuring cell. For the new cell construction the residual birefringence proved to be below the limit of detectability.

A simple test of the birefringence detection optics is a measurement on the reference substance water. The Kerr constant derived

from the observed amplitudes, $K_{\text{sp}} = 1.3 \times 10^{-20} \text{ m}^2 \text{ V}^{-2}$ (buffer T, 3 °C), is in reasonable agreement with literature values.^{12,13}

For comparison, it is useful to analyze the effects in a case where the birefringence is large. The case of a DNA restriction fragment with a chain length below the persistence length is useful, because the birefringence decay can be described by single exponentials.^{14,15} The test DNA with 84 base pairs showed a linear increase of the stationary amplitude $\Delta I/I$ with the square of the electric field strength E^2 up to $E \approx 5$ kV/cm, as expected in the Kerr law limit. At higher E -values there is a decrease of the $\Delta I/I$ -amplitude below the values expected by extrapolation of the Kerr law (Figure 4a). The slowest exponential τ_2 found in the birefringence decay shows a clear increase with increasing field strength E (the fast component τ_1 is due to the birefringence of water). This effect may be interpreted as field induced stretching of the DNA fragments.^{15,16} However, the change of the light intensity increases up to 60% in the case of high electric field

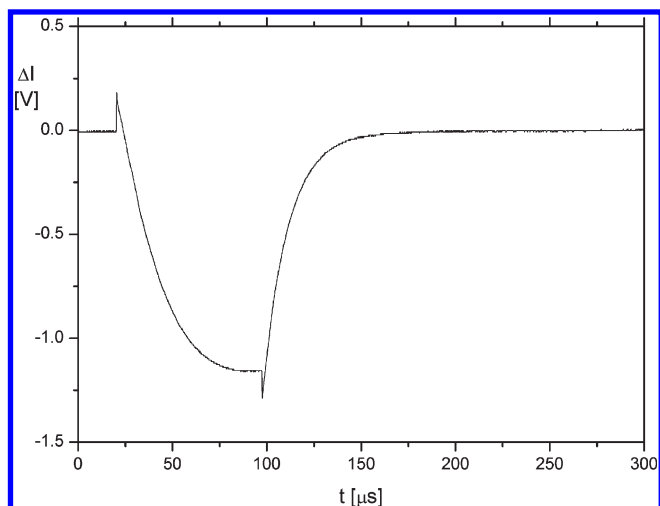


Figure 5. Birefringence transient ($\Delta I = f(t)$) of a DNA fragment with 549 base pairs in 70 mM NaCl, 35 mM Na-cacodylate pH 7, 0.2 mM EDTA at 2 °C. Electric field pulse of 1.15 kV/cm applied from 20.2 to 97.4 μ s, 56.6 nM helix concentration, average of 20 individual transients.

strengths. Thus, the transients are distorted to some extent. Conversion of these transients to values of the optical retardation based on eq 2 and exponential fitting provides time constants, which are independent of the electric field strength within the limit of experimental accuracy (cf. Figure 4b). Obviously, the same type of distortion affects the dependence of the amplitudes on the electric field strength. When stationary values in the form of the optical retardation are used, there is a linear dependence on the square of the electric field strength E^2 up to higher E -values (Figure 4a). Corresponding effects were observed for various DNA fragments, whenever the change of the light intensity due to birefringence exceeded values of $\sim 15\%$. These distortion effects could also be avoided simply by reduction of the DNA concentration.

The main goal of the construction was the extension of electric birefringence measurements to physiological salt concentrations. A simple example of a DNA fragment with 549 base pairs measured in a buffer containing 70 mM NaCl, 35 mM Na-cacodylate pH 7, 0.2 mM EDTA is given in Figure 5. The signal-to-noise ratio is much better than might have been expected under the given high salt conditions.

■ TOWARD THE LIMITS OF SENSITIVITY

The birefringence eq 2 predicts very high relative changes of light intensity, when the polarization plane of the analyzer is close to the crossed position. However, under these conditions birefringence transients may have a very complex shape, suggesting the existence of unusual processes. This is illustrated by a transient induced for a solution of a DNA restriction fragment with 256 base pairs by a pulse of low electric field strength (Figure 6a). It is well-known that under these conditions nothing special happens with the DNA double helix. The reason for the unusual shape is the fact that the optical retardation δ of the sample is negative and during pulse application the term $(\alpha + \delta/2)$ in eq 2 passes zero, leading to a minimum in the ΔI -values. Then the term $[\sin^2(\alpha + \delta/2) - \sin^2\alpha]$ passes zero, leading to $\Delta I = 0$, before ΔI increases to positive values. The unusual shape disappears, when the analyzer is rotated from its position with a

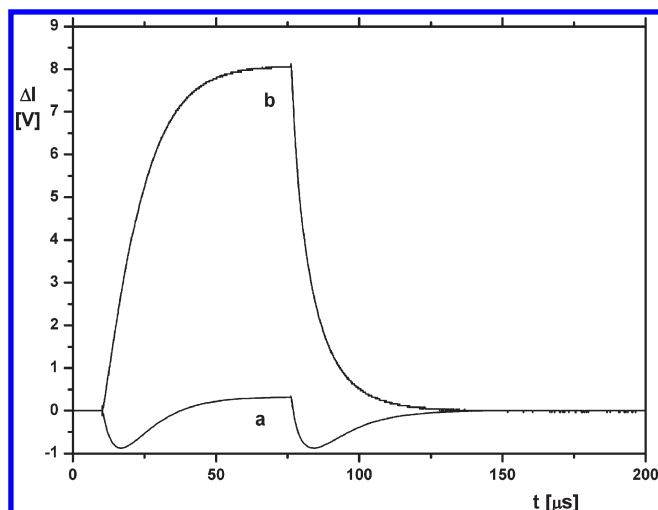


Figure 6. Birefringence transient ($\Delta I = f(t)$) of a DNA fragment with 256 base pairs in 1 mM NaCl, 1 mM Na-cacodylate, 0.1 mM Mg^{2+} at 2 °C; electric field pulse of 2.43 kV/cm applied from 10.1 to 76.0 μ s; helix concentration 0.114 μ M; average of 20 transients. Key: (a) polarization plane of the analyzer at $\alpha = +0.18^\circ$ from the crossed position and (b) $\alpha = -0.18^\circ$, i.e., to the opposite side from the crossed position.

positive α -value beyond the crossed position to a corresponding α -value but with a negative sign (cf. Figure 6b). This is consistent with the birefringence eq 2. Moreover, the experiment provides a verification of the huge relative change of the light intensity predicted by eq 2 under these conditions.

The extreme deformation of the transient observed at the positive α -value is avoided at the corresponding negative α -value, but nevertheless the observed change of the light intensity is not an exact linear function of the optical retardation in the second case either. Thus, fitting of decay time constants, for example, requires conversion of the $\Delta I/I$ -values to values of the optical retardation using eq 2. Fitting of the transient given in Figure 6b transformed to optical retardation provides a slow decay time constant consistent with expectation from measurements under conventional conditions.

■ DISCUSSION

The limits of the sensitivity are mainly determined by the magnitude of perturbations. One of the perturbations in birefringence measurements is the stray-light, defined as the light intensity passing through the polarizers in their crossed position and given relative to the light intensity passing in the parallel position of the polarizers. Because this stray-light does not contribute to the birefringence signal, the signal-to-noise ratio decreases with an increasing percentage of stray-light. The expression for an optimal setting of birefringence instruments^{11,17} according to $\sin(\alpha) = (K_{SL})^{1/2}$ is based on this fact, because the portion of stray-light would be too high at angles α below the value given by this relation. Thus, a decrease of K_{SL} opens up an extended range of favorable conditions for birefringence measurements. A discussion of “significant errors” arising when “optical component selection and setting are not critically considered”, has been presented by Jennings et al.¹⁸

However, even for perfect optical components and optimal alignment, perturbations of birefringence signals are not excluded completely. Shock waves induced by electric field pulses

may cause birefringence in the cell windows. Shock waves may be generated by volume expansion due to a field induced temperature increase and/or by electrostriction. The impact of the shock wave usually increases with the electric field strength. The detection limit is determined by the sensitivity.

These perturbations may be reduced to a minimum by selection of optimal boundary conditions. For aqueous solutions volume expansion is minimal at temperatures around the density maximum in the range of 0–4 °C. For salt concentrations in the range of 0.1 M, the optimal temperature turned out to be dependent even on the nature of the counterion (NaCl versus NaClO₄) and, thus, it is advisable to test for optimal conditions precisely, when a particularly high sensitivity is required.

The birefringence eq 2 predicts for the case of negative δ -values a rather complex dependence of $\Delta I_\delta/I_\alpha$ on α upon reducing α to the crossed position: the absolute value of $\Delta I_\delta/I_\alpha$ approaches a maximum at $\alpha = -\delta/2$, then goes through 0 at $\alpha = -\delta/4$ and the sign is reverted. Stellwagen¹³ measured $\Delta I_\delta = f(\alpha)$ at a constant input of laser light intensity and verified the existence of the zero-point at $\alpha = -\delta/4$. Equation 2 predicts a particularly high sensitivity at very low positive α -values for a positive birefringence and at very low negative α -values for a negative birefringence. The transient in Figure 6 illustrates the very large change of light intensity under these conditions. For large changes of $\Delta I/I$, it must be expected that these changes are not a linear function of the optical retardation anymore. Under these conditions, conversion of $\Delta I/I$ to optical retardation is required, which can be managed without problem by appropriate software.

Electro-Optical Anomalies. The electro-optical transient of a DNA fragment shown in Figure 6a has an unusual shape in spite of the fact that the optical retardation as a function of time is not unusual at all. This electro-optical anomaly can be avoided by turning the analyzer beyond the crossed position to “negative” angles α (Figure 6b). There are two other types of “unusual” transients observed for double helical DNA. In electro-optics the term “unusual” denotes transients with an inversion point indicating or suggesting changes in the sign of the birefringence or electric dichroism. Unusual transients have been observed for DNA under conditions, where the electric field induces denaturation of the double helix.^{19,20} Finally, a third case has been found, where the complex shape results from the contribution by a special quasi-permanent dipole moment in bent DNA fragments.^{21,22} Thus, there can be quite different reasons for the appearance of electro-optical transients with an “unusual” shape.

Laser Light Effects. The application of high light intensities for enhanced sensitivity of birefringence measurements may induce some side effects. First of all, there may be birefringence effects due to the electromagnetic field of the light itself. Effects of this type have been discussed by various authors.^{23–25} However, a critical experimental analysis by Wirth et al.²⁵ with particular emphasis on DNA double helices did not reveal any measurable effect. In the present investigation there was no evidence for light induced birefringence, using input laser light intensities up to 5 W in the given optical setup.

Another type of perturbation may result from laser trapping effects, which may lead to accumulation of macromolecules in the light beam and to aggregation. However, laser trapping is practiced for particles^{26,27} much larger than those used in standard studies of electric birefringence. The effects described in Figure 4b might be misinterpreted as evidence for a trapping effect, induced by a combined action of laser light and external

electric field. However, the quantitative analysis described above demonstrated that the changes of the decay time constants result from a nonlinearity in the relation between the change of light intensity and the birefringence. In summary, the present investigations did not show any evidence for the existence of laser trapping effects under the conditions of the current birefringence experiments.

Theory and Experiments. The special effects predicted by birefringence theory for the range of small angles from the crossed position have been discussed and tested previously only with respect to the point of zero optical response ($\Delta I_\delta/I_\alpha = 0$).¹³ The other special effects, including the divergent increase of $\Delta I_\delta/I_\alpha$ to extreme values and the electro-optical anomaly, have not been discussed or demonstrated previously, although these effects are of both practical and theoretical interest. The present measurements have been performed rather close to the divergence limit and the observed increase of relative amplitudes $\Delta I_\delta/I_\alpha$ is in agreement with predictions of the theory—within the limits of experimental accuracy. Furthermore, the experiments revealed a new type of electro-optical anomaly and a simple procedure to avoid this anomaly, again in agreement with the theory. Finally, deviations from linearity observed in the experiments are also in line with the theory. Deviations of experimental data from theoretical predictions may appear for very large optical retardations at angles close to the crossed position, because boundary conditions used in the theoretical derivation may be violated.

The new birefringence instrument proved to be particularly useful already in the analysis of biological macromolecules in solutions with physiological salt concentrations.^{28,29} Under these conditions the birefringence amplitudes are usually much smaller than those observed at low salt concentration and, thus, a particularly high sensitivity is required.

How far can the limits be extended? Further extension of the sensitivity under sufficiently well-defined conditions requires not only reduced stray-light constants but also polarizers of particularly high quality together with devices for more accurate adjustment/reading of angular positions of polarizers. A progress in the suppression of cell artifacts seems to be possible, for example by finding special types of glass, showing less birefringence under the action of pressure waves than quartz.

CONCLUSIONS

The theory of electric birefringence predicts that the relative birefringence amplitude diverges to extreme values at small angles from the crossed position. Extension of birefringence measurements into this neglected range with enhanced sensitivity requires light sources of high intensity and construction of cells with strain-free optical windows. Using a novel type of cell window together with selected optical components, the stray-light constant of an instrument for measurements of the electric birefringence has been reduced to 2×10^{-7} . A solid-state 532 nm laser with a light intensity in the range 0.5 to 5 W is applied for measurements at small angles α from the crossed position. The resulting increase of sensitivity and the advanced signal-to-noise ratio are particularly useful, e.g., for experiments at physiological salt. Special effects at small α are demonstrated, including a divergent increase of the relative optical effect, a nonlinear response for large birefringence amplitudes, a new type of electro-optical anomaly and a simple bypass around this anomaly. These effects are shown to be consistent with theory. Perturbations of measurements can be avoided by selection of optimal experimental conditions.

AUTHOR INFORMATION

Corresponding Author

*Telephone: -551-2011438. Fax: -551-2011168. E-mail: dpoersc@gwdg.de.

ACKNOWLEDGMENT

The author is indebted to Prof. Dr. Claude Houssier for information on the validity range of the birefringence equations. The expert support by Matthias Kleinhaus in the construction of the cell windows is gratefully acknowledged.

REFERENCES

- (1) Fredericq, E.; Houssier, C. *Electric dichroism and electric birefringence*; Clarendon Press: Oxford, U.K., 1973.
- (2) *Molecular Electro-Optics: Part 1 - Theory and Methods*; O'Konski, C. T., Ed.; Marcel Dekker: New York, 1976.
- (3) *Molecular Electro-Optics: Part 2 - Applications to Biopolymers*; O'Konski, C. T., Ed.; Marcel Dekker: New York, 1978.
- (4) Porschke, D.; Antosiewicz, J. M. Quantitative molecular electro-optics: Macromolecular structures and their dynamics in solution. In *Molecular and colloidal electro-optics*; Stoylov, S. P., Stoimenova, M. V., Eds.; CRC: Boca Raton, Fla., 2007; pp 59–107.
- (5) Porschke, D.; Obst, A. *Rev. Sci. Instrum.* **1991**, *62*, 818–820.
- (6) Porschke, D. *Biophys. Chem.* **1991**, *40*, 169–179.
- (7) Schonknecht, T.; Porschke, D. *Biophys. Chem.* **1996**, *58*, 21–28.
- (8) Porschke, D. *Ber. Bunsen-Ges. Phys. Chem.* **1996**, *100*, 715–720.
- (9) Porschke, D.; Jung, M. J. *Biomol. Struct. Dyn.* **1985**, *2*, 1173–1184.
- (10) Porschke, D.; Schmidt, E. R.; Hankeln, T.; Nolte, G.; Antosiewicz, J. *Biophys. Chem.* **1993**, *47*, 179–191.
- (11) Houssier, C.; O'Konski, C. T. Electro-Optical Instrumentation Systems with their Data Acquisition and Treatment. In *Molecular Electro-Optics*; Krause, S., Ed.; Plenum: New York, 1981; pp 309–339.
- (12) Orttung, W. H.; Meyers, J. A. *J. Phys. Chem.* **1963**, *67*, 1905–1910.
- (13) Stellwagen, N. J. *Phys. Chem.* **1989**, *93*, 7730–7732.
- (14) Elias, J. G.; Eden, D. *Macromolecules* **1981**, *14*, 410–419.
- (15) Diekmann, S.; Hillen, W.; Morgeneyer, B.; Wells, R. D.; Porschke, D. *Biophys. Chem.* **1982**, *15*, 263–270.
- (16) Porschke, D. *Biopolymers* **1989**, *28*, 1383–1396.
- (17) Newman, J.; Swinney, H. L. *Biopolymers* **1976**, *15*, 301–315.
- (18) Jennings, B. R.; Rudd, P. J.; Waterman, D. R. *J. Colloid Interface Sci.* **2005**, *288*, 304–307.
- (19) O'Konski, C. T.; Stellwagen, N. C. *Biophys. J.* **1965**, *5*, 607–613.
- (20) Diekmann, S.; Porschke, D. *Biophys. Chem.* **1982**, *16*, 261–267.
- (21) Antosiewicz, J.; Porschke, D. *Biophys. Chem.* **1989**, *33*, 19–30.
- (22) Porschke, D. *Colloids Surf., B: Biointerfaces* **2007**, *56*, 44–49.
- (23) Buckingham, A. D. *Proc. Phys. Soc. London, Sect. B* **1956**, *69*, 344–349.
- (24) Coles, H. J.; Jennings, B. R. *Biopolymers* **1975**, *14*, 2567–2575.
- (25) Wirth, M.; Eriksson, T.; Norden, B. *J. Phys. Chem.* **1987**, *91*, 1957–1960.
- (26) Chu, S. *Rev. Mod. Phys.* **1998**, *70*, 685–706.
- (27) Svoboda, K.; Block, S. M. *Annu. Rev. Biophys. Biomol. Struct.* **1994**, *23*, 247–285.
- (28) Porschke, D. *J. Phys. Chem. B* **2007**, *111*, 12004–12011.
- (29) Porschke, D. *Biochemistry* **2010**, *49*, 5553–5559.